Mode analysis with a spatial light modulator as a correlation filter

Daniel Flamm,[1,*] Darryl Naidoo,[2] Christian Schulze,[1] Andrew Forbes,[2,3] and Michael Duparré[1]

[1]*Institute of Applied Optics, Friedrich Schiller University Jena, Fröbelstieg 1, D-07743 Jena, Germany*

[2]*Council for Scientific and Industrial Research National Laser Centre, P.O. Box 395, Pretoria 0001, South Africa*

[3]*School of Physics, University of KwaZulu-Natal, Private Bag X54001, Durban 4000, South Africa*

**Corresponding author: daniel.flamm@uni-jena.de*

Received March 14, 2012; revised April 25, 2012; accepted April 30, 2012; posted May 1, 2012 (Doc. ID 164710); published June 19, 2012

A procedure for the real-time analysis of laser modes using a phase-only spatial light modulator is outlined. The procedure involves encoding into digital holograms by complex amplitude modulation a set of orthonormal basis functions into which the initial field is decomposed. This approach allows any function to be encoded and refreshed in real time (60 Hz). We implement a decomposition of guided modes propagating in optical fibers and show that we can successfully reconstruct the observed field with very high fidelity. © 2012 Optical Society of America

OCIS codes: 060.2270, 090.1995, 140.3295, 030.4070.

Techniques to achieve a full modal decomposition of light have been mooted for some time [1–3] and remain topical due to the physical insights offered from full knowledge of the field, for example, to study beam quality dynamics of laser resonators [4], beam quality degradation in high-power fiber lasers [5], and the orbital angular momentum structure of light [6,7]. Recently the correlation filter method (CFM) [4,8,9] has been demonstrated to retrieve the full information about the investigated optical field through measurement of only a few modal amplitudes and phases. To date, such optical correlation filters have been realized as amplitude-only or phase-only computer-generated holograms (CGHs) using corresponding coding techniques [10] being elaborately fabricated via laser lithography [8]. Though highly accurate measurement results have already been achieved using these types of CGHs [9,11], they exhibit an enormous disadvantage: a CGH that is endued with the spatial field information of a certain set of modes is limited to analyze only the corresponding type of fiber or resonator. This requires *a priori* knowledge of the field under investigation, both in terms of the modal basis and the scale parameters within this basis.

In this Letter we overcome this limitation by employing complex amplitude modulation encoded digital holograms on a liquid-crystal-on-silicon-based phase-only spatial light modulator (SLM). The advantages of replacing the stationary CGHs by flexible SLMs can be found in the rapid change of the transmission function and real-time switching of the digital holograms. Hence, with a single SLM, an arbitrary and unknown fiber or laser resonator can be investigated since the user is able to iteratively adapt the mode set for the decomposition, if, e.g, the exact fiber properties and thus the spatial information about the modes are unknown. Finally, the ubiquitous nature of SLMs nowadays in combination with a simple experimental setup makes the presented procedure outstandingly suitable for analyzing the modes of arbitrary laser beams.

By way of example, we consider the modal decomposition of an arbitrary field U into guided modes ψ_l in a conventional step-index fiber, where the linearly polarized (LP) basis set [12] is employed: $U(\mathbf{r}) = \sum_l \rho_l \exp(\mathrm{i}\phi_l)\psi_l(\mathbf{r})$. The modal weighting coefficients ρ_l may be found by inner product of the field with a suitable transmission function, $|\langle U|\psi_l^*\rangle| = \rho_l$, while the modal phases ϕ_l may be extracted by interference with a suitable reference mode [8]. The task is to encode the transmission function $T(\mathbf{r}) = \psi_l^*(\mathbf{r})$ onto the SLM by complex amplitude modulation. By using the technique proposed by Arrizón *et al.* [13], this complex valued function $T(\mathbf{r}) = A(\mathbf{r})\exp[\mathrm{i}\Phi(\mathbf{r})]$, with $A \in [0,1]$ and $\Phi \in [-\pi,\pi]$ is encoded into a phase hologram $H(\mathbf{r}) = \exp[\mathrm{i}\Psi(\mathbf{r})]$ with given unit amplitude transmittance and a certain phase modulation $\Psi(A,\Phi)$. In the literature, different phase modulations $\Psi(\mathbf{r})$ are discussed [10,13], providing the same information as the original transmission function $T(\mathbf{r})$ in a certain diffraction order. In this Letter we measure in the first order of diffraction and use $\Psi(A,\Phi) = f(A)\sin(\Phi)$, where $f(A)$ results from $J_1[f(A)] \cong 0.6A$, with the first-order Bessel function $J_1(x)$ [13]. As phase carrier we employed a sinusoidal grating with a spatial frequency of 8 line pairs/mm. The resulting phase modulations for measuring the modal power spectrum of the six lowest-order LP modes are depicted in Fig. 1.

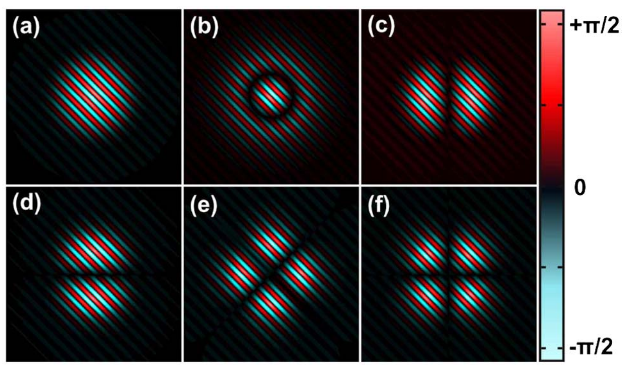

Fig. 1. (Color online) Encoded phase modulations $\Psi(\mathbf{r})$ for measuring the modal power of the six lowest-order LP modes guided in the step-index fiber under test. (a)–(f): LP_{01}, LP_{02}, LP_{11e}, LP_{11o}, LP_{21e}, LP_{21o}. Note that the required phase range for the SLM is merely $\cong 1.2\pi$ [13].

 © 2012 Optical Society of America

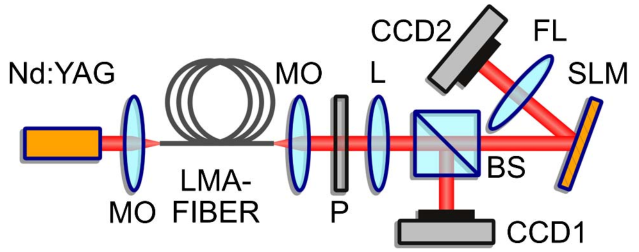

Fig. 2. (Color online) Schematic of the experimental setup. The SLM acts as a device for arbitrary complex amplitude modulation of the output modes from the fiber.

In our setup (Fig. 2) linearly polarized light from an Nd:YAG laser of wavelength $\lambda = 1064$ nm was coupled through a microscope objective (MO) into a large mode area (LMA) fiber (fiber A, $V = 4.7 \rightarrow 6$ guided LP modes; fiber B, $V = 2.7 \rightarrow 3$ guided LP modes). The output plane of the fiber was relay imaged through a beam splitter (BS), to a near-field CCD camera (CCD1) and a phase-only liquid-crystal-on-silicon SLM operating in reflection mode. The SLM (Holoeye, HEO1080-P with 1920×1080 pixels of pitch 8 μm and calibrated for a 2π phase shift at $\lambda = 1064$ nm) was programmed with a grayscale image containing the information about the transmission functions introduced in Fig. 1. The diffracted field from the SLM was Fourier transformed by lens FL and the signal detected on CCD2 where the intensities of the correlation channels were used to infer the modal composition. Care was taken to ensure that the correct linear polarization state was selected for a specific orientation of the SLM screen by use of a polarizer (P). The measurement results were achieved by utilizing the SLM's capability for switching its phase modulation with a frame rate of 60 Hz. Hence, the modal power spectrum was measured by successively implementing the transmission functions of Fig. 1 and analyzing the respective diffraction patterns.

In many cases, the fundamental mode operation of a fiber is of particular interest due to the high beam quality. In Fig. 3, the measurement and analyzing process of a fundamental mode-like beam emerging from fiber A is depicted schematically. Here Fig. 3(a) shows the corresponding measured near-field intensity of the beam that is illuminating the SLM. The resulting first-order diffraction patterns, also called "correlation answers," for measuring the modal amplitudes of the six guided modes are depicted in Figs. 3(b)–3(g). Note that the information of the modal amplitudes is directly measured on the optical axis of the diffracted signal (red crosses). In the case of a CCD camera, this corresponds to a single pixel. In this case, a noticeable intensity is only measurable on the optical axis of the correlation answer detecting the modal power of the fundamental mode. The resulting modal power spectrum shows that more than 97% of the total power is guided in the fundamental mode. By additionally measuring the phase differences of the guided modes to a chosen reference mode [8], the full field information about the investigated beam becomes available and allows for the reconstruction of the beam's intensity. Based on this information, it is our basic principle to compare the measured [Fig. 3(a)] and reconstructed intensities [Fig. 3(i)] to ensure the success of the measurement. In this case, the two-dimensional cross correlation coefficient C [14] of the two intensity signals is 0.98 attesting an excellent measurement result.

Figure 4 depicts the measurement result of modally decomposing a beam with higher-order mode content emerging from fiber A. We again measure successively the modal amplitudes of the six lowest-order LP modes using the transmission functions presented in Fig. 1. The resulting correlation answers are shown in Figs. 4(b)–4(g). Similar to the mode analyzing process of the fundamental mode-like beam, we again directly measure the modal power as intensity on the optical axis of the diffracted signal (red crosses). The resulting modal power spectrum [Fig. 4(h)] shows that ≈60% of the total power is guided by higher-order modes. The reconstruction of the beam's intensity becomes possible by additionally measuring the intermodal phase delays of the modes. A comparison of the measured [Fig. 4(a)] and reconstructed signals [Fig. 4(i)] again confirms the quality of the measurement process ($C = 0.96$).

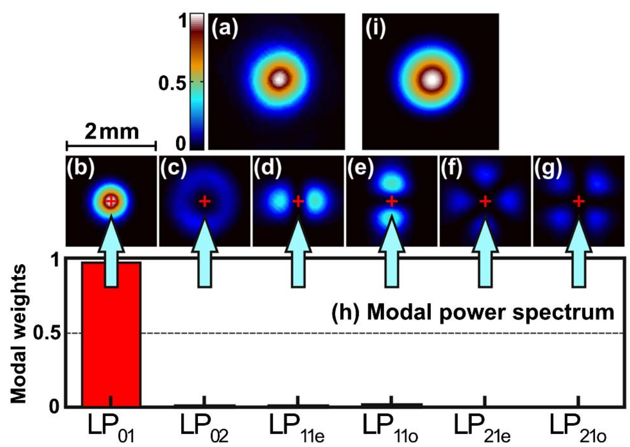

Fig. 3. (Color online) Mode analysis of a fundamental mode-like beam. (a) Measured near-field intensity. (b)–(g) Correlation answers using the six transmission functions of Fig. 1. (h) Measured modal power spectrum. (i) Resulting reconstructed near-field intensity.

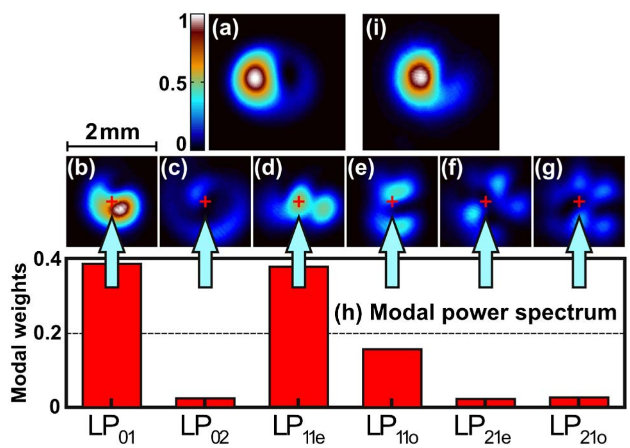

Fig. 4. (Color online) Mode analysis of a beam with higher-order mode content. (a) Measured near-field intensity. (b)–(g) Correlation answers using the six transmission functions of Fig. 1. (h) Measured modal power spectrum. (i) Resulting reconstructed near-field intensity.

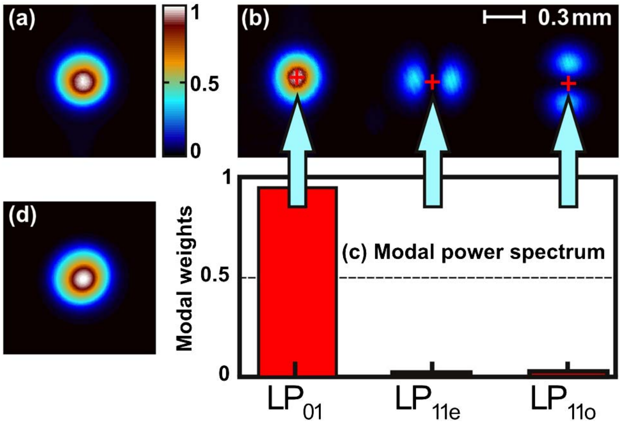

Fig. 5. (Color online) Mode analysis of a fundamental mode-like beam. (a) Measured near-field intensity. (b) Spatially separated correlation answers using the multiplexing technique. (c) Measured modal power spectrum. (d) Resulting reconstructed near-field intensity.

As already pointed out, it is a basic advantage of the CFM to perform real-time measurements, while the information about modal amplitudes and intermodal phase differences is directly accessible as an intensity signal; no further numerical evaluation is necessary. In the case of employing an SLM as the correlation filter, the comparatively large pixel pitch limits the implementation of high-carrier frequencies and, thus, the number of multiplexed transmission functions that can be encoded. For this reason, the measurements leading to the results depicted in Figs. 3 and 4 have been achieved by successively implementing the respective transmission functions onto the SLM. The temporal effort of the measurements presented here is in the range of some seconds and is limited by the automation control between camera and SLM, but in principle the SLM used in this study can refresh at rates of 60 Hz. If there is only a small number of modes to be investigated, then the multiplexing technique [8] can also be applied to the SLM successfully so that the measurement rate is increased significantly. By using the conventional CCD cameras of our setup, we are able to monitor the model amplitudes of few mode fibers simultaneously with rates of 15 Hz. This ability is shown here exemplarily for analyzing a fundamental mode-like beam guided from fiber B. In Fig. 5(a)we plotted the measured near-field intensity. A detail of the corresponding diffraction pattern is depicted in Fig. 5(b) and shows the spatially separated correlation answers recorded simultaneously for measuring the modal amplitudes of the three guided LP modes. At the same time, we measured the intermodal phase differences of the higher-order modes to the fundamental mode by implementing four additional transmission functions [8]. However, for reasons of space, the corresponding correlation answers of the phase measurements are not shown here. The modal power spectrum measured from the single camera recording and the resulting reconstructed near-field intensity can be seen in Figs. 5(c) and 5(d), respectively. The maximum number of multiplexed transmission functions will strongly depend on the type of fiber. In the case of step-index fibers with comparatively smooth mode profiles, up to five modal amplitudes can be measured simultaneously using the specified SLM.

To conclude, we have introduced a versatile measurement procedure that employs digital holograms by complex amplitude modulation as correlation filters for the modal decomposition of arbitrary laser sources. We have demonstrated the efficacy of this approach by successfully decomposing the guided modes of a step-index fiber into the LP basis functions using a phase-only SLM as the encoding device and then reconstructing the near-field pattern from the resulting modal weights and phases. The reconstructed intensities are in very good agreement with the experimentally measured patterns. This technique can be used to as a tool to study passive fibers and fiber lasers, superposition fields carrying orbital angular momentum for classical and quantum applications, and as a mode demultiplexing scheme in future telecommunication systems.

References

1. O. Shapira, A. F. Abouraddy, J. D. Joannopoulos, and Y. Fink, Phys. Rev. Lett. **94**, 143902 (2005).
2. J. W. Nicholson, A. D. Yablon, S. Ramachandran, and S. Ghalmi, Opt. Express **16**, 7233 (2008).
3. N. Andermahr, T. Theeg, and C. Fallnich, Appl. Phys. B **91**, 353 (2008).
4. O. A. Schmidt, C. Schulze, D. Flamm, R. Brüning, T. Kaiser, S. Schröter, and M. Duparré, Opt. Express **19**, 6741 (2011).
5. F. Stutzki, H.-J. Otto, F. Jansen, C. Gaida, C. Jauregui, J. Limpert, and A. Tünnermann, Opt. Lett. **36**, 4572 (2011).
6. I. A. Litvin, A. Dudley, and A. Forbes, Opt. Express **19**, 16760 (2011).
7. A. Dudley, I. A. Litvin, and A. Forbes, Appl. Opt. **51**, 823 (2012).
8. T. Kaiser, D. Flamm, S. Schröter, and M. Duparré, Opt. Express **17**, 9347 (2009).
9. D. Flamm, C. Schulze, R. Brüning, O. A. Schmidt, T. Kaiser, S. Schröter, and M. Duparré, Appl. Opt. **51**, 987 (2012).
10. J. P. Kirk and A. L. Jones, J. Opt. Soc. Am. **61**, 1023 (1971).
11. D. Flamm, O. A. Schmidt, C. Schulze, J. Borchardt, T. Kaiser, S. Schröter, and M. Duparré, Opt. Lett. **35**, 3429 (2010).
12. D. Gloge, Appl. Opt. **10**, 2252 (1971).
13. V. Arrizón, U. Ruiz, R. Carrada, and L. A. González, J. Opt. Soc. Am. A **24**, 3500 (2007).
14. C. Schulze, O. A. Schmidt, D. Flamm, S. Schröter, and M. Duparré, Proc. SPIE **7914**, 79142H (2011).